Synthesis of 9-(4-nitrophenylsulfonyl)-9H-Carbazole: Comparison of an Impedance Study of Poly[9-(4-nitrophenylsulfonyl)-9H-carbazole] on Gold and Carbon Fiber Microelectrodes

Murat Ates, Nesimi Uludag

Department of Chemistry, Faculty of Arts and Sciences, Namik Kemal University, Degirmenalti Campus, 59030 Tekirdag, Turkey

ABSTRACT: In this study, 9-(4-nitrophenylsulfonyl)-9H-carbazole (NPhSCz) monomer was chemically synthesized. The monomer characterization was performed by Fourier transform infrared spectroscopy, ^{1}H-NMR, and melting point analysis. Two different electropolymerizations of NPhSCz were studied on a gold microelectrode (Au electrode) and carbon fiber microelectrodes (CFMEs) in a 0.1M sodium perchlorate (NaClO$_4$)/acetonitrile solution. The electropolymerization experiments were done from 1 to 4 mM. The characterizations of two different modified electrodes of poly[9-(4-nitrophenylsulfonyl)-9H-carbazole] [poly(NPhSCz)] were performed by various techniques, including cyclic voltammetry, scanning electron microscopy–energy-dispersive X-ray analysis, and electrochemical impedance spectroscopy (EIS). The effects of the initial monomer concentrations (1, 2, 3, and 4 mM) were examined by EIS. The capacitive behaviors of the modified electrodes were defined via Nyquist, Bode magnitude, Bode phase, and admittance plots. The variation of the low-frequency capacitance (C_{LF}) and double-layer capacitance (C_{dl}) values are presented at different initial monomer concentrations. Poly(NPhSCz)/CFME was more capacitive ($C_{LF} = 6.66$ F/cm^2 and $C_{dl} \approx 28$ mF) than the Au electrode ($C_{LF} = 6.53$ F/cm^2 and $C_{dl} \approx 20$ mF). An equivalent circuit model of R[QR(CR)(RW)](CR), (R: Current, Q: Constant phase element, C: Double layer capacitance, W: Warburg impedance), was used to fit the theoretical and experimental data. © 2011 Wiley Periodicals, Inc. J Appl Polym Sci 124: 4655–4662, 2012

Key words: coatings; fibers; redox polymers; synthesis; thin films

INTRODUCTION

Conducting polymers (CPs) have been a subject of intense investigation by many research groups worldwide. During the past decade, there have been many articles related to CPs; these have led to practical applications in various areas, such as batteries, sensors, antistatic coatings, and supercapacitors.[1–3] Electrochemical impedance spectroscopy (EIS)[4,5] has been used to study the electrical properties of thin films of electroactive CPs.[6] The functional groups in the modified polymers open the possibility of using such electrocoated polymers serving as electrochemical capacitors.[7–9] In previous studies, the electropolymerization of carbazole derivatives was examined with various functional groups, such as the anionic polymerization of 4-(9-carbazolyl) methyl styrene,[10] poly(N-alkyl-3,6-carbazoles),[11] poly[9-(4-vinylbenzyl)-9H-carbazole],[12] poly(N-hydroxyl methyl carbazole),[13] poly(N-vinyl carbazole),[14] poly(9-tosyl-9H-carbazole-co-pyrrole),[15] 5-(3,6-dibromo-9H-carbazole-9-yl) pen-

tane nitrile,[16] poly(9-benzyl-9H-carbazole),[17] and poly(9-tosyl-9H-carbazole).[18]

Carbon fibers have present extremely high strength and modulus values, good stiffness, creep resistance, and so on.[19] The application of a polymeric interface acting as a coupling agent can improve the interfacial properties between reinforcing carbon fiber microelectrodes (CFMEs) and the polymeric matrix.[20] The surfaces of coated CFMEs have been characterized by electrochemical characterization techniques.[21–24]

In this article, the synthesis of 9-(4-nitrophenylsulfonyl)-9H-carbazole (NPhSCz) and its characterization were presented by Fourier transform infrared (FTIR) spectroscopy, ^{1}H-NMR, and melting point analysis. The modified poly[9-(4-nitrophenylsulfonyl)-9H-carbazole] [poly(NPhSCz)] on a gold electrode and CFME was characterized in different initial monomer concentrations by cyclic voltammetry (CV), FTIR–attenuated total reflection (ATR) spectroscopy, scanning electron microscopy (SEM)–energy-dispersive X-ray analysis (EDX), and EIS. Poly(NPhSCz) on a gold electrode and CFME thin films were synthesized in the equivalent circuit model of R[QR(CR)(RW)](CR), where R: Current, Q: Constant phase element, C: Double layer capacitance, W: Warburg impedance.
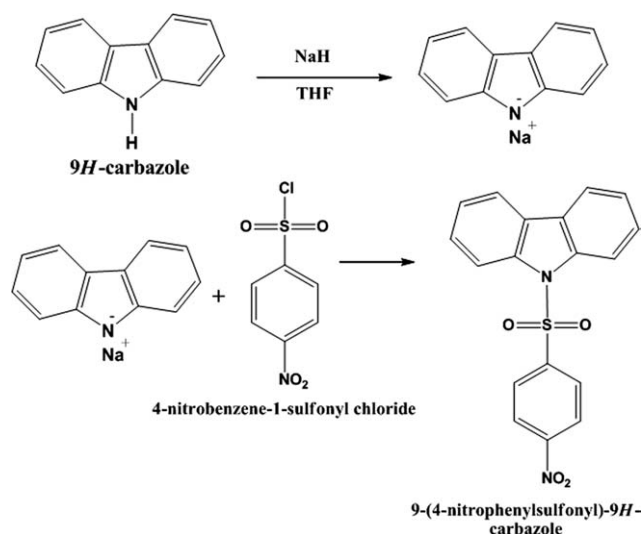
Figure 1 Synthesis method of the NPhSCz monomer.

EXPERIMENTAL

Materials

Carbazole (>98%), 4-nitrobenzene-1-sulfonyl chloride (>95%), tetramethyl ammonium hydrogen sulfate, and sodium perchlorate (>98%) were obtained from Sigma-Aldrich (Munich, Germany). Dichloromethane, silica gel (60 F254), acetonitrile (ACN), sodium hydride, hydrochloric acid, sodium hydroxide, ethyl acetate, and tetrahydrofuran were purchased from Merck (Darmstadt, Germany). All chemicals were high-grade reagents and were used as received.
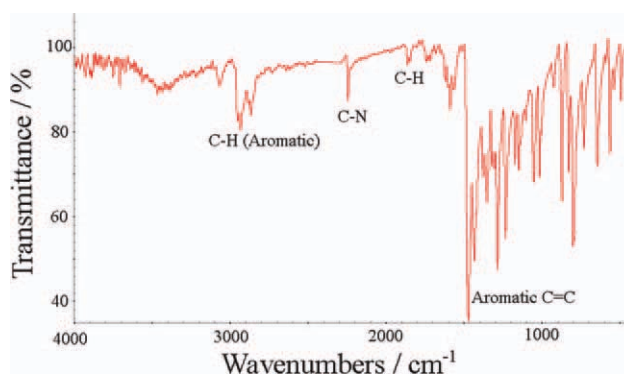

Figure 2 FTIR spectrum of the synthesized NPhSCz monomer. [Color figure can be viewed in the online issue, which is available at wileyonlinelibrary.com.]

Instrumentation

The ^{1}H-NMR (400-MHz) spectrum was recorded with a Bruker DPX-400 (Bremen, Germany) 400-MHz high-performance digital Fourier transform NMR spectrometer with $CDCl_3$ at room temperature. Chemical shifts are expressed in terms of parts per million (δ), and the coupling constants are given in hertz. IR spectra were recorded with a Mattson 1000 FTIR spectrometer (East coast, USA) as KBr pellets. The melting points were determined in a capillary tube on an Electro thermal IA 9000, Electrothermal Engineering Ltd, Essex, UK apparatus. The reactions were monitored by thin-layer chromatography (silica gel 60 F254, Minneapolis, USA). The purification of solvents was performed according to standard methods.
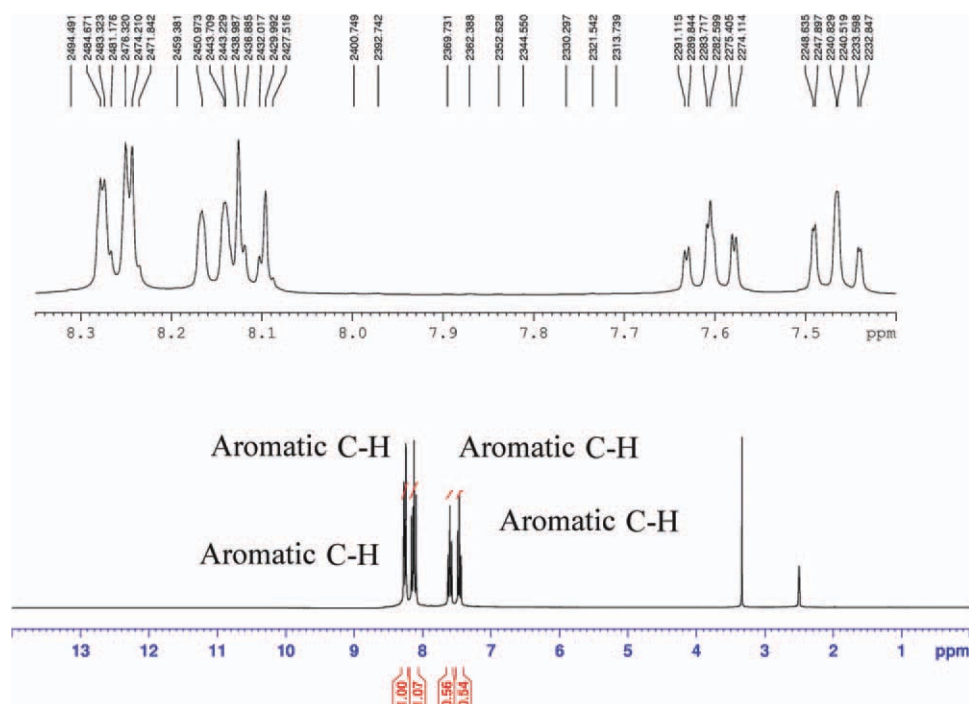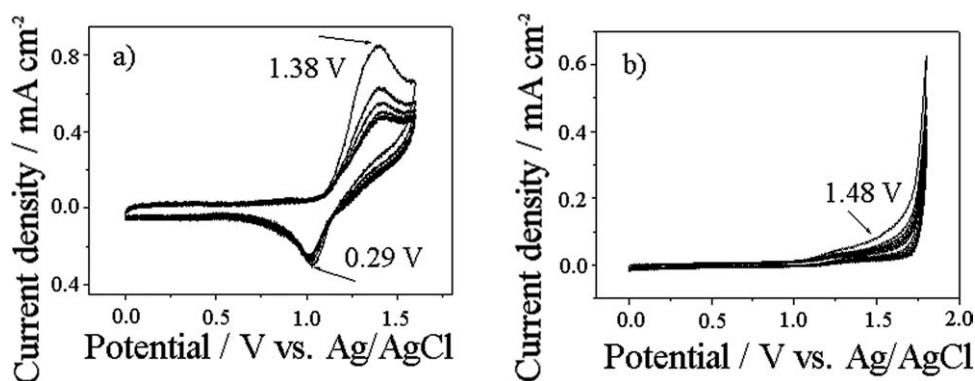

Figure 3 ^{1}H-NMR ($CDCl_3$, 400 MHz) spectrum of the synthesized NPhSCz monomer. [Color figure can be viewed in the online issue, which is available at wileyonlinelibrary.com.]

Figure 4 Electrogrowth of poly(NPhSCz). Polymerization conditions: (a) $Q = 422.0$ μC on the Au microelectrode and (b) $Q = 4.1$ mC on CFME, $[NPhSCz]_0 = 2$ mM, scan rate = 100 mV/s, eight cycles, in $0.1M$ NaClO$_4$/ACN.

CV was performed with a PARSTAT 2263–1 (PowerSuite software and Faraday cage, BAS Cell Stand C$_3$, IN, USA) in a three-electrode electrochemical cell with a CFME or gold electrode as the working electrodes, platinum wire as the counter electrode, and Ag/AgCl as the reference electrode. A gold disc electrode (diameter = 10 μm, area of gold electrode = 3.14×10^{-6} cm^2) prepared with gold wire assembled in a glass tube with epoxy resin was used as the working electrode.

Electrocoated CFMEs were characterized by FTIR reflectance spectroscopy (PerkinElmer, Spectrum One B, with an ATR attachment Universal ATR with a ZnSe crystal, C70951, Massachusetts, USA). Modified CFMEs were washed in a solvent of ACN.

CFME preparation

High-strength and high-modulus carbon fibers (C320.000A, CA, Sigri Carbon, Meitengen, Germany) containing 320,000 single filaments in a roving were used as working electrodes. All of the electrodes were prepared with a 3 cm long bundle of the CFME (with an average diameter of around 7 μm) attached to a copper wire with a Teflon tape. The number of carbon fibers in the bundle were about 10. One centimeter of the CFME was dipped into the solution to keep the electrode area constant (∼ 0.022 cm^2), and the rest of the electrode was covered with Teflon tape. The CFMEs were first cleaned with acetone and then dried with an air dryer before the experiments.

TABLE I
Charges during the Electrodeposition Process of Poly(NPhSCz) on the Au Electrode and CFME

| $[NPhSCz]_0$ (mM)	Au electrode (mC)	CFME (mC)
1	7.89	0.79
2	18.04	0.78
3	52.74	0.70
4	14.16	0.81

Synthesis of NPhSCz

Carbazole (3.0 g, 19.45 mmol) and 4-nitrobenzene-1-sulfonyl chloride (8.6 g, 38.91 mmol) were dissolved in dichloromethane (300 mL); tetramethyl ammonium hydrogen sulfate (0.3 g) and sodium hydroxide (40 mL, 50%) were added to this solution. The mixture was stirred at room temperature for 24 h. Then, the mixture was poured into water and dichloromethane. The solvent was evaporated, and the residue was purified by silica gel chromatography and crystallized from ethyl acetate. NPhSCz (4.7 g, 74%) was obtained with the following properties: melting point = 193°C and molecular weight = 352.05 g/mol. The synthesis method is given in Figure 1.

IR (potassium bromide, Fig. 2, ν, cm^{-1}): 3100 (aromatic C—H), 1950 (aliphatic C—H), 1609, 1451, 1329 (aromatic C=C). ^{1}H-NMR (deuteriochloroform, Fig. 3, δ): 8.3–8.2 (d, 4H, aromatic CH), 8.2–8.05 (m, 3H, aromatic CH), 7.6 (m, 2H, aromatic CH), 7.5–7.3 (m, 2H, aromatic CH). ANAL. Calculated for C$_{18}$H$_{12}$N$_2$O$_4$S (352.05): C, 61.36%; H, 3.44%; N, 7.93%. Found: C, 61.39%; H, 3.41%; N, 7.97%.
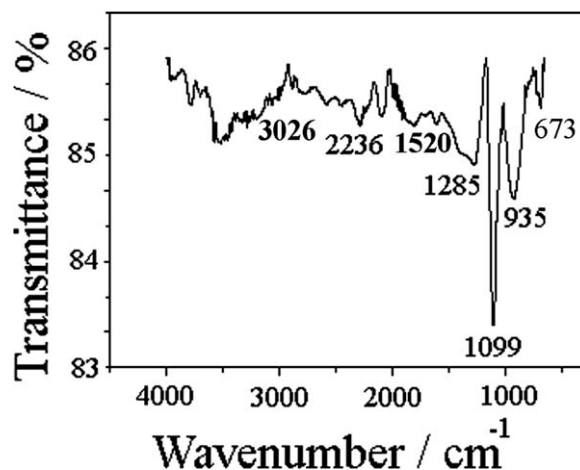
Figure 5 FTIR–ATR spectrum of poly(NPhSCz)/CFME, $Q = 4.1$ mC, $[NPhSCz]_0 = 2$ mM, scan rate = 100 mV/s, eight cycles, in $0.1M$ NaClO$_4$/ACN.
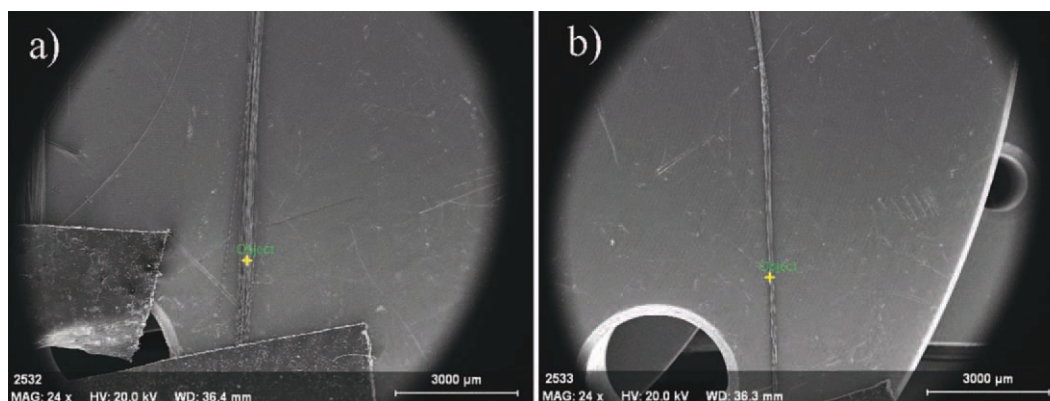
Figure 6 SEM measurement of poly(NPhSCz) on the end part of carbon fiber: $[NPhSCz]_0$ = (a) 2 and (b) 4 mM. [Color figure can be viewed in the online issue, which is available at wileyonlinelibrary.com.]

EIS

EIS measurements were taken at room temperature (23 ± 2°C) with a conventional three-electrode cell configuration. EIS measurements were conducted in monomer-free electrolyte solution with a perturbation amplitude of 10 mV over a frequency range of 10 mHz to 100 kHz with PARSTAT 2263–1 (Power-Suite software).

RESULTS AND DISCUSSION

Electropolymerization of NPhSCz on CFMEs

The electropolymerization process was achieved by the CV method at a scan rate of 100 mV/s. The electrogrowth of NPhSCz on the gold electrode and CFME is shown in Figure 4(a,b). Electropolymerization experiments were done containing 0.1M $NaClO_4$/ACN in different initial monomer concentrations from 1 to 4 mM in the potential range 0.0–1.6 V at room temperature. The anodic and cathodic peak potentials were affected by the variation of initial monomer concentrations. Thus, we suggest that this reaction was irreversible for the gold electrode and CFME. The oxidation peak potentials were obtained as 1.38 and 1.48 V for the gold electrode and CFME, respectively. In the first CV cycle, the anodic peak appearing at 1.38 V for $[NPhSCz]_0$ = 2 mM was attributed to the radical cation formation of NPhSCz. There was a slight potential shift of NPhSCz compared to the carbazole radical (1.4 V, charge density = 70.5 mC/cm^2) in previous studies.[25]
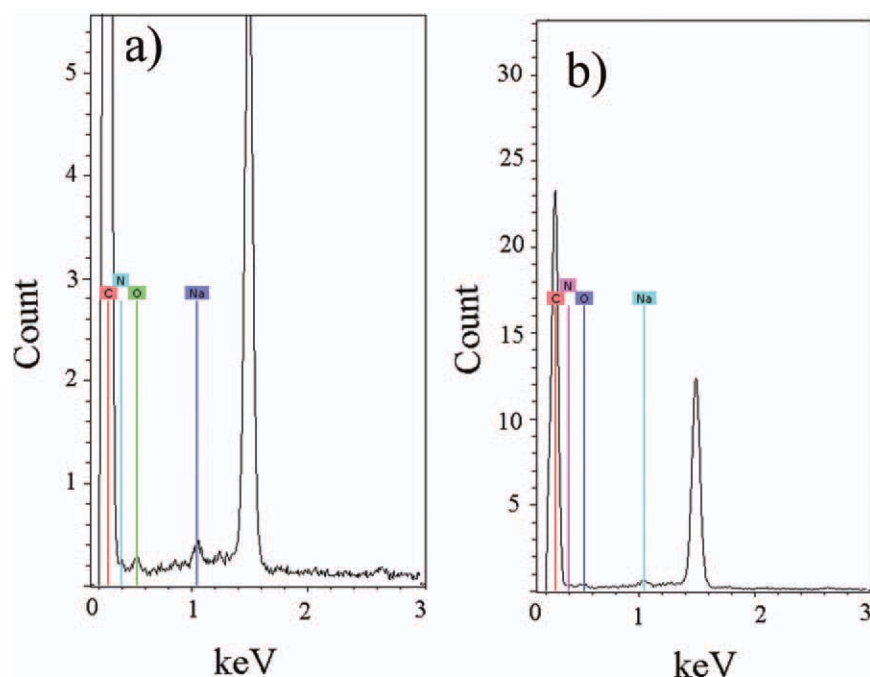
Figure 7 EDX measurement of poly(NPhSCz) on the end part of carbon fiber: $[NPhSCz]_0$ = (a) 2 and (b) 4 mM. [Color figure can be viewed in the online issue, which is available at wileyonlinelibrary.com.]

TABLE II
EDX Measurements of Poly(NPhSCz)/CFME with
Different Initial Monomer Concentrations

[NPhSCz]$_0$ (mM)	Element			
	C (%)	N (%)	O (%)	Na (%)
1	65.13	17.11	16.51	1.25
2	59.91	18.78	19.58	1.73
3	69.49	15.79	13.52	1.20
4	59.24	18.11	20.31	1.34

The electrogrowth process of poly(NPhSCz) began to take place.

The peak separation between the anodic and cathodic peak potentials (ΔE) during polymer growth was obtained on a gold microelectrode as 1.09 V for [NPhSCz]$_0$ = 2 mM. The anodic and cathodic peak current density ratio was closer to that at 2.83. The most coated thin film was obtained from an electrogrowth process (Q = 422.0 µC). Therefore, these data indicated that the irreversible redox behavior on the gold electrode coated at an initial monomer concentration of 2 mM. ΔE is associated with ion-transport resistance involved in these redox reactions.[26] It gives information about the polymer thickness; that is, if the polymer thickness is high, electron transfer between the polymer and electrolyte will be slow. Thus, ΔE can serve as an indication for resistance of ion migration in the electrode. The highest charges were obtained for the Au electrode and CFME during the electrogrowth process (Table I).

FTIR–ATR measurements of poly(NPhSCz)/CFME

The FTIR–reflectance spectra of electrocoated poly(NPhSCz) prepared under the given experimental conditions are shown in Figure 5. The band at 1099 cm^{-1} was attributed to perchlorate ion, which was due to the electrolyte in NaClO$_4$.[27,28] The peaks were observed at 3026 cm^{-1} (aromatic CH stretching), 1520 cm^{-1} (aromatic N—O peaks), 1285 cm^{-1} (antisymmetric stress vibration of the S=O bond),[29] 935

cm^{-1} (—C—H out of plane deformation of C—H bond in benzene ring), and 673 cm^{-1} (C=CH bond). The bond located at 2236 cm^{-1} was confirmed by valance vibration of the C—N bond of the carbazole cycle.[30]

### SEM–EDX measurements of electrocoated poly(NPhSCz)/CFME

The morphological features of the modified electrode on CFME were performed for [NPhSCz]$_0$ = 2 and 4 mM by SEM analysis [Fig. 6(a,b)]. The fibers were attached to a copper plate by use of double-sided carbon tape. The morphology of carbon fiber (CF) itself exhibited a smooth surface with a surface curvature, and the morphology of the polymer films were clearly dependent on the initial monomer concentration; this indicated that electron transfer to the electrode was a factor that could be used to control the surface morphology. The high-resolution images obtained by SEM analysis of the electrocoated CFMEs showed that the electropolymerization of conductive polymers with different initial monomer concentrations (2 and 4 mM) produced different sized grainy orientations.

EDX measurements (Fig. 7) were obtained at various initial monomer concentrations, as shown in Table II. The highest Na element (1.73%) and N element (18.78%) were obtained for [NPhSCz]$_0$ = 2 mM.

EIS study

All of the electrodes showed a slight deviation from the capacitive line (y axis); this indicated fast charge transfer at the gold electrode and CFME/polymer/solution interfaces and fast charge transport in the polymer bulk. The increase in steepness in Nyquist plot is shown in Figure 8.

The Nyquist plot for poly(NPhSCz) indicated the highest low-frequency capacitive behavior (C_{LF}) at a frequency of 10 mHz at an initial monomer
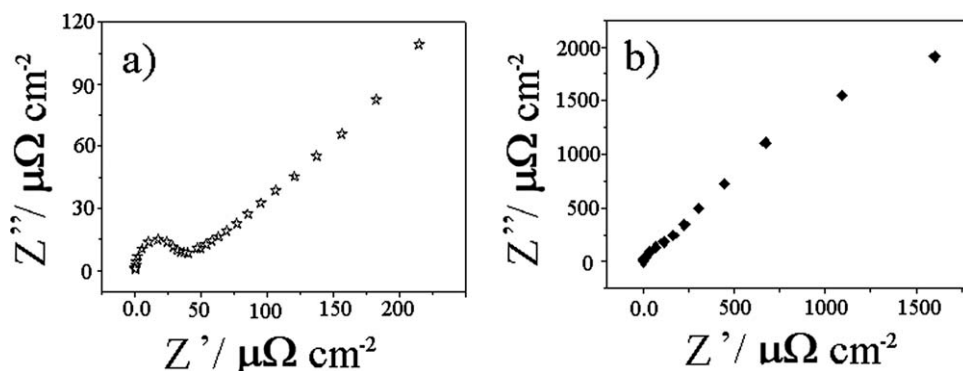
Figure 8 Nyquist plots for poly(NPhSCz) electrocoated on (a) the Au electrode and (b) CFMEs ([NPhSCz]$_0$ = 1 mM). (Z': real impedance vs. Z'': imaginary impedance).
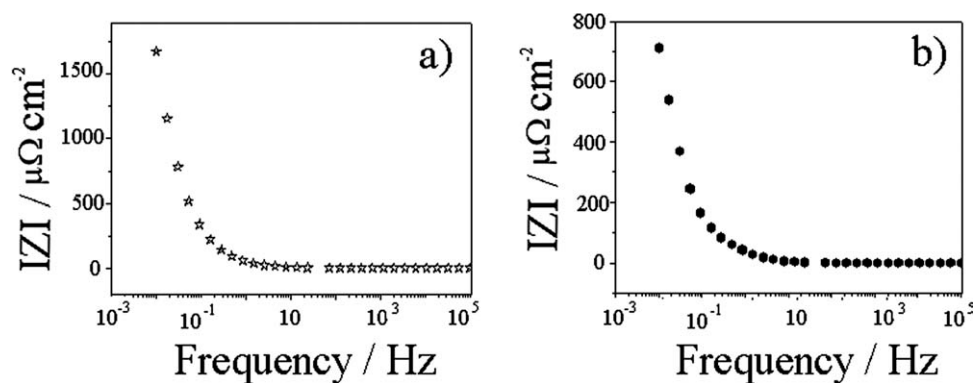
Figure 9 Bode magnitude plots of the poly(NPhSCz) electrocoated on (a) the Au electrode and (b) CFMEs. $[NPhSCz]_0 =$ 2 mM.

concentration of 2 mM. C_{LF} was obtained as 6.53 and 6.66 F/cm^2 on Au and CFME, respectively. The lowest frequency and the highest imaginary impedance (Z_{im} or z'') values were placed in the formula $C_{LF} = 1/2\pi f z''$ for C_{LF} calculations.

A value of the double-layer capacitance (C_{dl}) could be calculated from a Bode magnitude plot by extrapolation of the linear section to a value of ω of 1 (log w = 0), where ω = 2 × π × f and f is the frequency, with the relationship IZI = $1/C_{dl}$, as shown in Figure 9. The magnitude IZI represents the ratio of the voltage difference amplitude to the current amplitude, while the angle □ gives the phase difference between voltage and current. The C_{dl} values were obtained as about 20 and 28 mF for the gold electrode and CFME, respectively.

At high frequencies, the magnitude of the impedance of such a cell is equal to a phase angle of 0°. At low frequencies, the impedance will be frequency-dependent, and the phase angle will be 90°. At the maximum phase angle for poly(NPhSCz) on the Au electrode and CFME, the impedance was obtained as between about 77.5 and 82.8° at a frequency of 10^2

Hz. However, the lower phase angles (ca. 72.3 and 55.9°) were obtained for $[NPhSCz]_0 = 2$ mM at a frequency of 0.27 Hz, as given in Figure 10.

The highest conductive polymer was obtained on the Au electrode ($Y'' = 232.27$ mS/cm^2; Fig. 11). The other conductivity result was obtained on CFME as $Y'' = 118.91$ mS/cm^2 for $NaClO_4$/ACN. Y = Z^{-1}; Y is the admittance (S), Z is the impedance (Ω).

The electrochemical parameters of the gold electrode and CFME/poly(NPhSCz)/electrolyte system were evaluated by the ZSimpWin programe, Michigan, USA. The Kramers–Kronig test yielded values for the χ^2 which means the sum of the squares of the difference between the calculated and experimental values of the real and imaginary impedances. From the correlation results, when χ^2 was observed as minimized below 10^{-4}, χ^2 was the function defined as the sum of the squares of the residuals. In all cases, the experimental data were compared to an equivalent circuit that used some of the conventional circuit elements, namely, the resistances (R_s, R_1, R_2, R_3, and R_4, where R_s is the solution resistance), capacitance values of the double layers (C_1
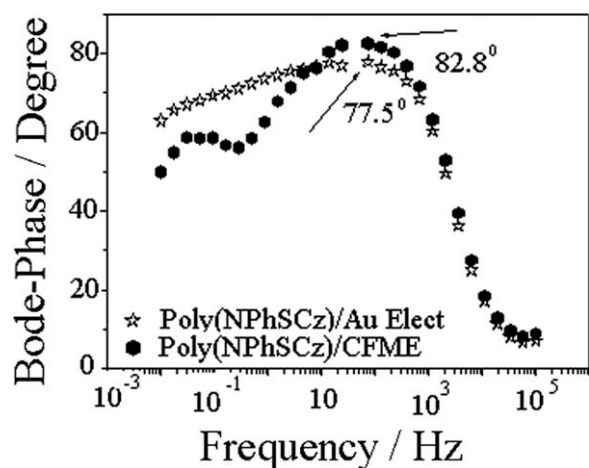
Figure 10 Bode phase plot of poly(NPhSCz) electrocoated on (a) the Au electrode and (b) CFMEs. $[NPhSCz]_0 =$ 2 mM.
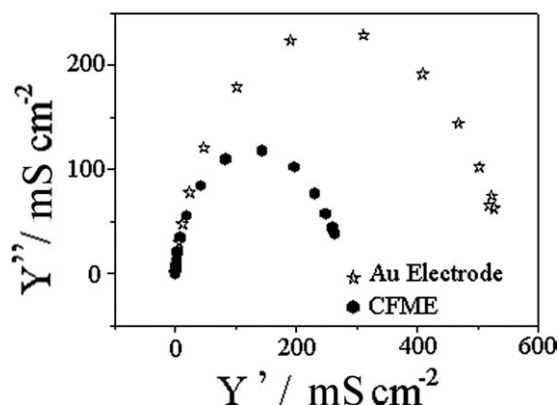
Figure 11 Admittance plot of poly(NPhSCz) electrocoated on (a) the Au electrode and (b) CFMEs. $[NPhSCz]_0$ = 2 mM.
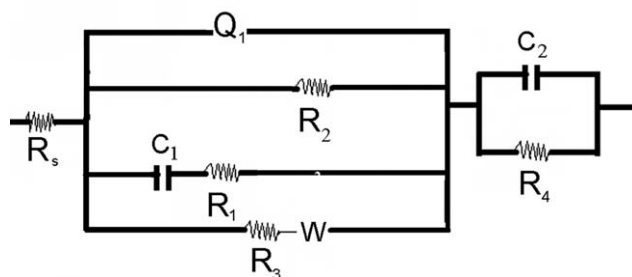
Figure 12 Circuit model of R[QR(CR)(RW)](CR).

and C_2), Warburg impedance (W) and induction elements in the circuit of R[QR(CR)(RW)](CR) (Fig. 12).

Capacitors in EIS experiments often do not behave ideally; instead, they act like a constant phase element (Q_1). Diffusion can create impedance, known as *Warburg impedance* (W).[31] The Warburg element is easily recognized by a line with an angle of 45° in the lower frequency region. R_s is almost within the limits of the experimental errors. In other words, the ionic/electronic charge-transfer resistance (Q_1) shows a gradual increase and then a decrease in the value within the applied potential indicating that the migration of ionic species within the film pores is not the only means of change–exchange at the polymer/electrolyte interface.[32] When the charge transfer is also influenced by diffusion to and from the electrode, the Warburg impedance will be seen in the impedance plot. At solid electrodes, C_{dl} shows a phase angle of less than 90°. The impedance of such a nonideal double layer is represented by $Z = -j/(\omega \times Q_1)^n$, Z is complex impedance notation ($Z = Z' + jZ''$ with $j = \sqrt{-1}$), ω is angular frequency. This element is called the constant phase element (Q_1). For ideal electrodes, $Q_1 = C_{dl}$ and $n = 1$. Usually, n has values between 0.5 and 1. This effect is supposed to be due to surface roughness or is caused by heterogeneity of the surface. In our EIS results, n was obtained as 0.95 for CFME. The constant phase element ($Q_1 = 1.45 \times 10^{-7}$) and C_{dl} (C_1

TABLE III
EIS Results of Poly(NPhSCz) on the Au Electrode and CFME by Means of the Circuit Model R[QR(CR)(RW)](CR)

Circuit component	Polymer on the Au electrode	Polymer on CFME
χ^2	1.3×10^{-4}	6.89×10^{-4}
R_s (Ω)	153.2	262.9
Q (F)	1.22×10^{-6}	1.45×10^{-7}
n	0.70	0.95
R_1 (Ω)	2.3×10^8	1.08×10^8
C_1 (F)	1.48×10^{-7}	1.5×10^{-7}
R_2 (Ω)	57.13	61.5
R_3 (Ω)	1×10^5	6.43×10^5
W ($\Omega/s^{1/2}$)	1.55×10^{-7}	1.62×10^{-7}
C_2 (F)	2.96×10^{-9}	1.1×10^{-9}
R_4 (Ω)	269.9	340.3

$= 1.5 \times 10^{-7}$) values were nearly the same, so poly(NPhSCz)/CFME was more ideal than the poly(NPhSCz)/gold electrode. The circuit elements could be compared, as shown in Table III.

CONCLUSIONS

In this study, the NPhSCz monomer was newly synthesized chemically. The monomer characterization was obtained by FTIR analysis and ^{1}H-NMR spectroscopy. Polymer characterizations of poly(NPhSCz) on the Au electrode and CFME were performed via CV, SEM–EDX, and EIS analysis. The thicker film ($Q = 422.0$ μC on the Au electrode and $Q = 4.1$ mC on CFME) at an initial monomer concentration of 2 mM had the highest C_{LF} values ($C_{LF} = 6.53$ F/cm^2 for the gold electrode and $C_{LF} = 6.66$ F/cm^2 for CFME) and C_{dl} values ($C_{dl} \approx 20$ mF for the gold electrode and $C_{dl} \approx 28$ mF for CFME). Poly(NPhSCz)/CFME was more capacitive than the poly(NPhSCz)/Au microelectrode. An equivalent circuit model of R[QR(CR)(RW)](CR) was used to fit the theoretical and experimental data.

References

1. Malinauskas, A. Polymer 2001, 42, 3957.
2. Liu, Q.; Nayfeh, M. H.; Yau, S-T. J Power Sources 2010, 195, 3956.
3. Ma, Y.; Yang, X. J Electroanal Chem 2005, 580, 348.
4. Sarac, A. S.; Sezgin, S.; Ates, M.; Turhan, C. M. Adv Polym Technol 2009, 28, 120.
5. Ates, M.; Sarac, A. S. Prog Org Coat 2009, 65, 281.
6. Vorotyntsev, M. A.; Badiali, J.-P.; Inzelt, G. J Electroanal Chem 1999, 472, 7.
7. Ates, M. Fibers Polym 2010, 11, 1094.
8. Liu, X.; Osaka, T. J Electrochem Soc 1997, 144, 3066.
9. Biniak, S.; Dzielendziak, B.; Siedlewski, J. Carbon 1995, 33, 1255.
10. Cho, Y.-S.; Kim, S.-W.; Ihn, C.-S.; Lee, J.-S. Polymer 2011, 42, 7611.
11. Lmimouni, K.; Legrand, C.; Legrand, A. Synth Met 1998, 97, 151.
12. Ates, M.; Uludag, N. Fibers Polym 2010, 11, 331.
13. Sarac, A. S.; Parlak, E. A.; Serhatli, E.; Cakir, T. J Appl Polym Sci 2007, 104, 238.
14. Ates, M.; Sarac, A. S. J Appl Electrochem 2009, 39, 2043.
15. Ates, M.; Uludag, N.; Sarac, A. S. Mater Chem Phys 2011, 127, 120.
16. Uludag, N.; Ates, M.; Tercan, B.; Hökelek, T. Acta Cryst 2011, E67, o642.
17. Uludag, N.; Ates, M.; Tercan, B.; Ermis, E.; Hökelek, T. Acta Cryst 2010, E66, o1077.
18. Ates, M.; Uludag, N.; Sarac, A. S. Fibers Polym 2011, 12, 8.
19. Donnet, J. B.; Bansal, R. C. Carbon Fibers, 2nd ed.; Dekker: New York, 1990.
20. Park, J. M.; Kim, Y. M.; Yoon, D. J. J Colloid Interface Sci 2000, 231, 114.
21. Sarac, A. S.; Springer, J. Surf Coat Tech 2002, 160, 227.
22. Sarac, A. S.; Evans, U.; Serantoni, M.; Clohessy, J.; Cunnane, V. J. Surf Coat Tech 2004, 182, 7.

23. Sarac, A. S.; Syed, T.; Serantoni, M.; Henry, J.; Cunnane, V. J.; McMonagle, J. B. Appl Surf Sci 2004, 222, 148.
24. Jamal, M.; Magner, E.; Sarac, A. S. Sens Actuators 2004, 97, 59.
25. Abe, S. Y.; Bernede, J. C.; Ugalde, L.; Tragouet, Y.; Del Valle, M. A. J Appl Polym Sci 2007, 106, 1568.
26. Tranvan, F.; Henri, T.; Chevrot, C. Electrochim Acta 2002, 47, 2927.
27. Zotti, G.; Zecchin, S.; Schiavan, G.; Seraglia, R.; Berlin, A.; Canavesi, A. Chem Mater 1994, 6, 1742.
28. Papez, V.; Ingonas, O.; Cimrova, V.; Nespurek, S. J Electroanal Chem Interfacial Electrochem 1990, 282, 123.
29. Kham, K.; Sadki, S.; Chevrot, C. Synth Met 2004, 145, 135.
30. Sarac, A. S.; Ates, M.; Parlak, E. A.; Turcu, E. F. J Electrochem Soc 2007, 154, D283.
31. Atta, N. F.; El-Kady, M. F. Talanta 2009, 79, 639.
32. Atta, N. F.; Galal, A.; Khalifa, F, Appl Surf Sci 2007, 253, 4273.